

3D Printed Smart Mold for Sand Casting: Monitoring Pre-Pour Binder Curing

Nathaniel Bryant¹, Janely Villela², Juan Owen Villela², Alan Alemán³,
Josh O'Dell¹, Sairam Ravi¹, Jerry Thiel¹, Eric MacDonald²

¹ Metal Casting Center, The University of Northern Iowa, Waterloo, IA, USA 50614

² The University of Texas at El Paso, TX USA 79902

³ Tec de Juárez, Ciudad Juárez, México

Abstract: *The benefits of additive manufacturing for fabricating complex sacrificial sand molds for geometrically-complex metal castings is revolutionizing the foundry industry driven by a digital manufacturing paradigm. The design freedom of 3D printing allows for new mold designs - not possible with traditional approaches - such as helical sprues, varying wall thickness to tailor the thermal history, and spatially-varying lattice castings. However, research on the curing time of printed molds, including the aging of printed molds, requires more exploration. This study describes the experimental evaluation of 3D printed specimens in which embedded environmental sensors were fully encapsulated into sand blocks during an interruption of the binder jetting process. Subsequently, over a 28 day duration, humidity, volatile organic compound generation, temperature and barometric pressure were captured for three environmental treatments. Mechanical testing of standard test specimens subjected to the same conditions was conducted. The sand structures held in high (uncontrolled) humidity and at reduced temperature were statistically significantly weaker than a third treatment based on the hypothesis that high humidity and/or low temperatures impede curing. The use of embedded sensors could provide guidelines for mold and core storage conditions as well as in high-value production to inform the minimum (for full curing) and maximum duration (mold expiration) after printing to identify the optimal time to pour metal during the life of a printed sand mold.*

Keywords: Additive Manufacturing; 3D Printed Sand Casting; Binder Jetting; Curing;

1.0 Introduction

Traditional sand casting is an economical metal manufacturing process that has been employed for thousands of years [1] and when compared to other casting processes (e.g. die casting, investment casting, etc.), sand casting can serve a diversity of alloys and can accommodate large casting structures. As the most common form of casting, sand casting produced over 100 million metric tons [2] of structures in 2020 [3]. Additive manufacturing is now being explored to generate sand molds and cores with complex and customized geometries with binder jetting [4] - one of the seven sub processes within the additive manufacturing taxonomy [5]. A serendipitous benefit of additive manufacturing is access between the printing of layers to insert components inside of the mold and new strategies are now possible in the design, ventilation (channels to

improve permeability), gating (sprues, runners to reduce the velocity of the molten metal to mitigate turbulence and reduce porosity [6]), and risers to manipulate the solidification.

3D printing of sacrificial molds and cores involves binder jetting in which a binder is selectively inkjetted into a bed of sand premixed with an acid to provide the two-part Furan curing reaction. After one layer of binder is jetted, the bed descends by a layer thickness (typically 250 microns) and a new layer of unbound sand is deposited uniformly across the bed and the process repeats. Interrupting the process and gaining access to the bed (either manually in this case, but potentially eventually with integrated robotics) is possible with ExOne SMAX printer and the capability to integrate components (e.g. chills, thermal conduits, electronics with sensors, actuation for dynamic gating systems, etc.), and subsequently, to continue the process to construct smart molds is now possible and relatively unexplored. Sand printing has been investigated at least preliminarily with explorations of the sand and binder materials [7–9], final casting characteristics such as porosity and surface finish [4,10,11], multiple-material castings [12,13], casting modeling [14], complex casting geometries [15–19] and even embedded sensors in molds and cores for unprecedented process monitoring [20,21] for detection of core shifts with sensitive and miniaturized accelerometers and gyroscopes [22], proper ventilation in molten-metal-engulfed cores [23] and even cyber security for the 3D print of sand molds [24].

The present effort has investigated the insertion of fully embedded sensors into 3D printed sand structures during process interruptions in the binder jetting of Furan-based sand molds. The driving hypothesis is that humidity and temperature (independent input variables) could be correlated to volatile organic compound production (dependent variable) and finally to the mold strength at the time of the metal pour. As potential future experiments may include extended durations (one year or more) of data collection and reporting, small Linux computers were employed that were not embedded in the structure to avoid the use of batteries as required by fully isolated sensor systems, thus allowing for virtually endless data collection. A recently developed and commercially-available four-mode sensor was inserted into a mold cavity that was exposed during a binder jetting interruption. A thin channel for a four-conductor cable allowed a Grove sensor connector to exit the structure but with minimal exposure of the internal sensor to the out-of-mold ambient conditions. Pressure, temperature, humidity and volatile organic compounds (VOC) were measured: temperature and humidity were considered control variables that directly impacted the effectiveness of the curing. VOCs were considered to be a product of the curing process and an indication of the extent of curing and a predictor of final mold strength. Barometric pressure was not expected to be of utility but provided an indication of the local weather which impacted the independent variables in the uncontrolled ambient treatment.

2.0 Materials and Methods

An industrial standard sand printer was used with traditional powder and binder consumables. The process was interrupted and a portal was accessed to directly and manually manipulate the printed sand structures in mid-fabrication for the integration of sensors in the structure

2.1 Printer and Binder

Test specimens were produced using an ExOne S-Max 3D sand printer (**Figure 1**) utilizing an 80 AFS-GFN round grain silica sand and a furan binder system. The recipe employed a 65% virgin / 35% recycled sand mixture and an activator dosage level of 0.17% based on the batch weight. This dosage level was contingent on the observed flowability of the sand during the layering process. The voxel dimensions used in this experiment were 0.1mm x 0.1016mm x 0.28mm, which resulted in a resin content of 1.2 - 1.25%, as determined by loss on ignition testing.



Figure 1: ExOne Sand Printer at the University of Northern Iowa

2.2 Test Specimens and Sand Block with Embedded Sensors

Test specimens were produced using an ExOne S-Max 3D sand printer utilizing an 80 AFS-GFN round grain to create cubes 75 mm on a side. In the center of the cube was a cavity that was larger in dimensions than the BME680 Grove sensor board and a small channel was introduced

from the internal cavity to the outside to allow for the exit of a 300 mm long Grove connector cable. The sensor location within the block was centered to maintain at least 75 mm of bound sand in all directions with the exception of the cable channel. In addition, with each block of twelve sand blocks, several flexural test specimens were included in both the Y axis (in direction of the powder recoating) and X axis (in direction with the inkjetting) based on AFS method 3348-18-S. These specimens were treated in the same manner as the sensorized blocks for the 28 day period. **Figure 2** illustrates the sand blocks during the process interruption (left) and after completion (right).

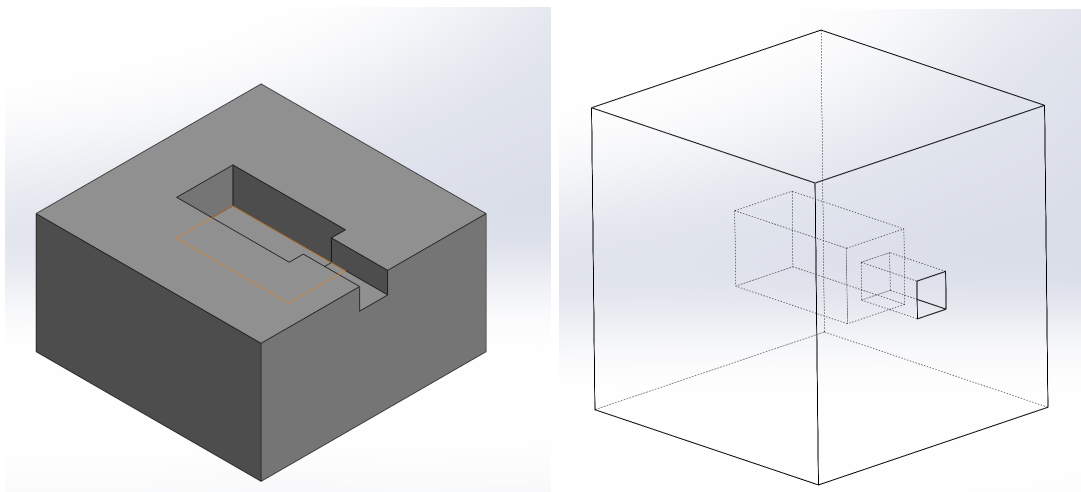


Figure 2: Sand block design at interruption (left) and after completion (right).

2.3 Experimental Treatments

Of the 12 sand blocks, sets of four (with two Raspberry PIs reading a pair of sensors each based on a limitation of the I2C bus addressing with a Grove Pi Hat used to connect the sensors) were subjected to three experimental treatments. **Table 1** describes the conditions for each treatment. The hypothesis of the experiment is that temperature and humidity would impede binder curing and reduce mechanical strength. The ambient treatment was to simulate a typical foundry scenario with changes in weather. Furthermore, volatile organic compounds were hypothesized to be an indication of binder curing completeness as an output of the chemical reaction. Volatile organic compounds are released in the process and the integral of measured VOCs could correlate with final binder strength and used to ensure that molds and cores can withstand the head pressure for the specific alloy, design and height to ensure casting quality and yield. The intent of the sensor monitoring was to ensure both that (1) molds have had sufficient time to cure (minimum time before pour after print) and (2) eventually to measure how long a mold can be stored in a warehouse or foundry before the binder begins to degrade and lose strength (maximum time between print and pour) for a given set of ambient conditions.

Table 1: Experimental treatments

Group Number	Conditions	Purpose
1 (four samples)	Laboratory ambient conditions to investigate a typical usage case of sand molds and cores.	Ambient environment in a lab in Iowa during April of 2022 with varying conditions.
2 (four samples)	Refrigerated environment	Constant low humidity and low temperature (nom 2 °C).
3 (four samples)	Oven at 35 °C	Constant low humidity and warm temperature (nom 35 °C)

2.4 Sensor Insertion Methodology

As the sand blocks were printed in the sand bed and at the point in which side walls of the internal cavity were complete and still accessible, the printer was interrupted and the loose sand in the cavities and channels were evacuated. The sensors were inserted with cables and additional unbound sand was backfilled into the remaining volume of the cavities to provide a flush sand surface upon which printing could resume. The printing process was restarted to finish the top half of the sand cube and to entrap the sensor inside the structure while maintaining electrical connections through the external four-conductor cable. The main requirement was that only unbound sand be higher than the recoating level to avoid leaving voids in the sand bed..

2.5 Standard Flexural Strength Testing

All test specimens were tested for both the X and Y axis according to AFS method 3349-18-S for flexural strength. The resultant stress was calculated from the measured load using equation 1.

$$\sigma = \frac{3FL}{bd^2} \quad \text{Eq. 1}$$

Where F is the measured load required to break the specimen, L is the span length, and the denominator (bd^2) is the cross-sectional area of the specimen.

3.0 Results and Discussion

The twelve blocks were binder jetted and a time lapse video of the sensor insertion process is shown here (**Video 1**). For a total of 28 days, data was collected. This effort and future work in long duration experiments are expected to provide guidelines for the storage of molds with minimum and maximum durations for a given set of humidity and temperature conditions. However, as these sensors are inexpensive, the utility of using these sensors even in production environments is possible and could help ensure the quality and yield of high-value castings. **Figure 3** shows how the sensors and cables are inserted through a printer portal in an evacuated cavity and channel.



Figure 3: Insertion of sensors and cables into the blocks during printer interruption.

3.1 Sensor insertion

Of the twelve blocks, one block on the second layer after reinitiating the printing process had a sensor lift above the powder bed level causing an obstruction during the subsequent powder recoating. A large, gaping hole remained as shown in [Video 1](#) and the half-built block and recoater collided. The cavity in the sand bed was manually backfilled with sand to allow for printing the top half of the block separately. After harvesting as shown in the video, the two detached sections of the bad block were manually bound together after inserting the sensor. This manually reconstructed block was included in the oven treatment and did not appear to have significantly different VOC behavior. **Figure 4** depicts the harvesting with sensors embedded and the cables exiting the sand blocks. Finally, **Figure 5** illustrates all six PIs reading 12 sensors directly after harvesting and just prior to subjecting the sand blocks to one of three treatments.



Figure 4: Harvesting of sand blocks with sensor cables shown.

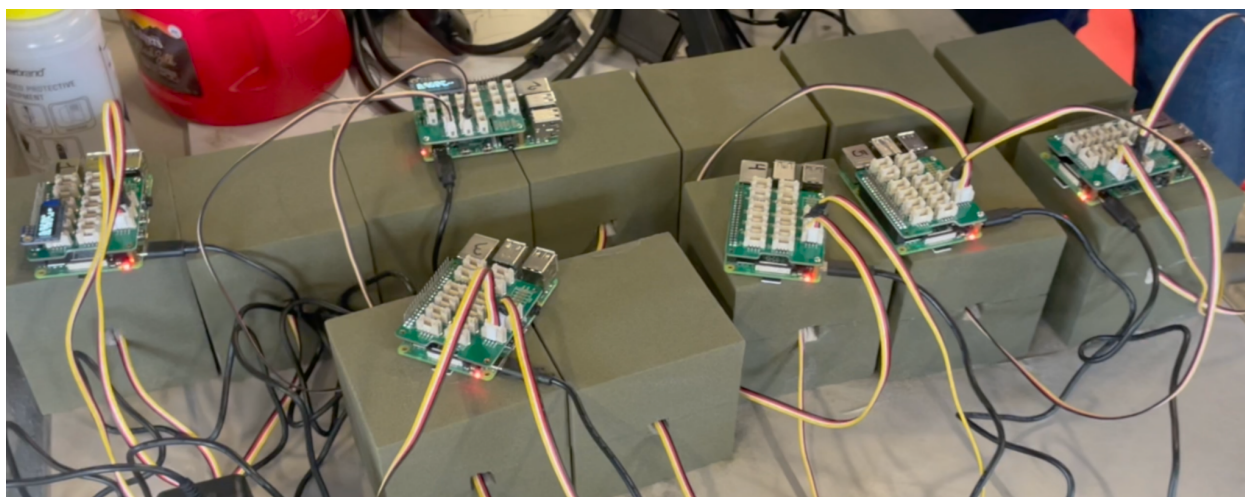


Figure 5: 12 Sand blocks and sensors connected to six Raspberry PIs prior to being subjected to the three environmental treatments.

3.2 Sensor data and the impact of local weather on curing

For 28 days, humidity, temperature, volatile organic compounds and barometric pressure were collected every minute. Although barometric data was not expected to provide utility in this investigation, one interesting discovery was that insights into the local weather and the potential impact on the binder curing of the blocks were uncovered. On day two of the duration, a snow storm descended upon Iowa and was manifested by a precipitous drop in the barometric pressure. During the period of reduced pressure, the humidity was shown to spike given the weather change and increased moisture in the air appears to have interfered with the production of volatile organic compounds. Of the experimental treatments, the case of ambient conditions would include the effect of this one-day duration of increased humidity as shown in **Figure 6**.

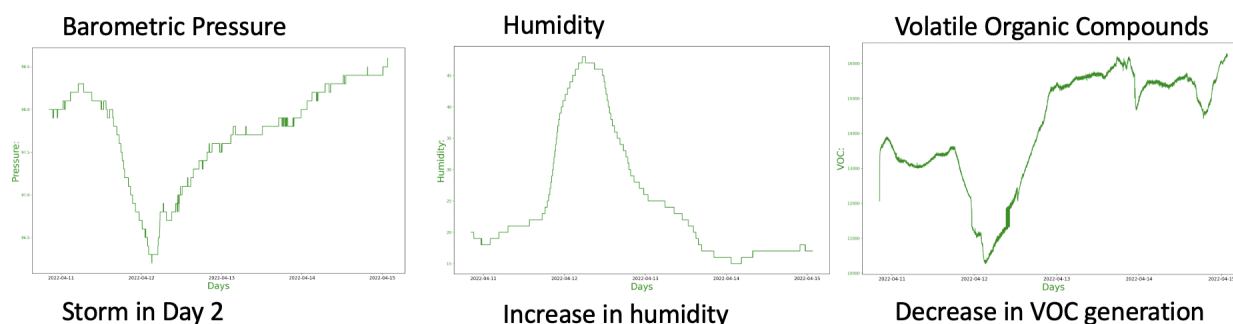


Figure 6: Barometric pressure (left), humidity (center) and VOC generation (right) of one ambient sensor is shown in which a snow storm was responsible for a local increase in humidity which is hypothesized to have reduced the VOC generation and thus impeded the curing process for approximately a day.

3.3 Sensor data for entire duration

Of the three treatments, four sensors were read from a pair of Raspberry Pi 4's each. However, for two of the Pis (one in the refrigerated treatment and another in the ambient treatment), sensor communication stopped even though WIFI communication with the Pis continued. An investigation for this failure is underway and the reason is unclear. Both sensors associated with each of the Pis was not readable so it appears to be related to the Pis; however, all six Pis with 12 sensors were tested for over a month prior to the sensors being embedded in sand and all collected data continuously and correctly. The only difference was that the sensors were subsequently embedded in acid-soaked sand but in the case of both non-functioning Pis, the two sensors were unreadable leading the investigators to believe that the sensors were not the problem (i.e. if related to the sensor functionality, only one would stop functioning). One possible explanation is that the sensors drew more power based on a resistive short between nodes on the board due to the moist sand and the increased power consumption caused a voltage droop in the Pis and affected the PI functionality.

Figure 7 illustrates the temperature, humidity and VOC generation for the four sensors in the oven treatment (low humidity and higher temperature). As expected, the temperature was measured between 34 and 38 °C and the humidity was maintained below 25% for the entire duration and all four sensors provided consistent data. The VOC generation was maintained at a level of between 20,000 and 40,000 ohms which served as a proxy for the actual VOCs and provided a relative level which was generally consistent throughout the duration with a slight increase over time. In all four sensors, two spikes are seen at approximately day 5 and 16 which correlated with unexpected power outages. The Pis were programmed to restart data collection if rebooted and the VOC sensor requires warming up with initial values that artificially spike for the first 30 seconds. The spikes provided additional information as an actual spike in VOC generation would generally last longer and the artificial spikes inform the user of a power outage or related reboot.

The VOC trends for all four sensors are consistent but the absolute values vary widely as these sensors were not calibrated. Consequently, without a calibration, these values cannot be used other than identify trends during the duration within a single mold and are not suitable for providing a final single metric value to indicate that the molds were sufficiently cured. Alternatively, the temperature and humidity values were consistent in terms of absolute value and together could be combined to provide a “pour / no pour” metric. The VOC sensors could be calibrated prior to use by measuring VOCs in a known VOC environment for a specific time. However, the temperature and humidity sensors are calibrated sufficiently out-of-the-box and could be used to calculate a single combined metric to determine the extent of the binder curing.



Figure 7: Oven treatment sensor data for four sensors read by two PIs.

The two sensors monitored in the refrigerated treatment are shown in **Figure 8** with temperature and humidity both as expected. The initial temperature is higher as the sensors were connected in the laboratory and later transported to the refrigerator causing an initial higher temperature. Only two sensors were included in this treatment as one of PIs stopped reading the additional two sensors. Similarly to the oven treatment, the conditions were consistent for the cold, low-but-slightly higher humidity case than the oven treatment. The VOCs in both cases appear to have a slow declining trend in value and although the shape of the graphs are very similar and show the power outage that was seen in the oven treatment data, the overall magnitudes of the graphs differ by a factor of three by the end of the experiment, further illustrating how the absolute values for this sensor is not valid but rather that the general trend for any given sensor may provide insights. In this case, different from the oven treatment, the VOCs appear to slowly decline over the 28 day period.

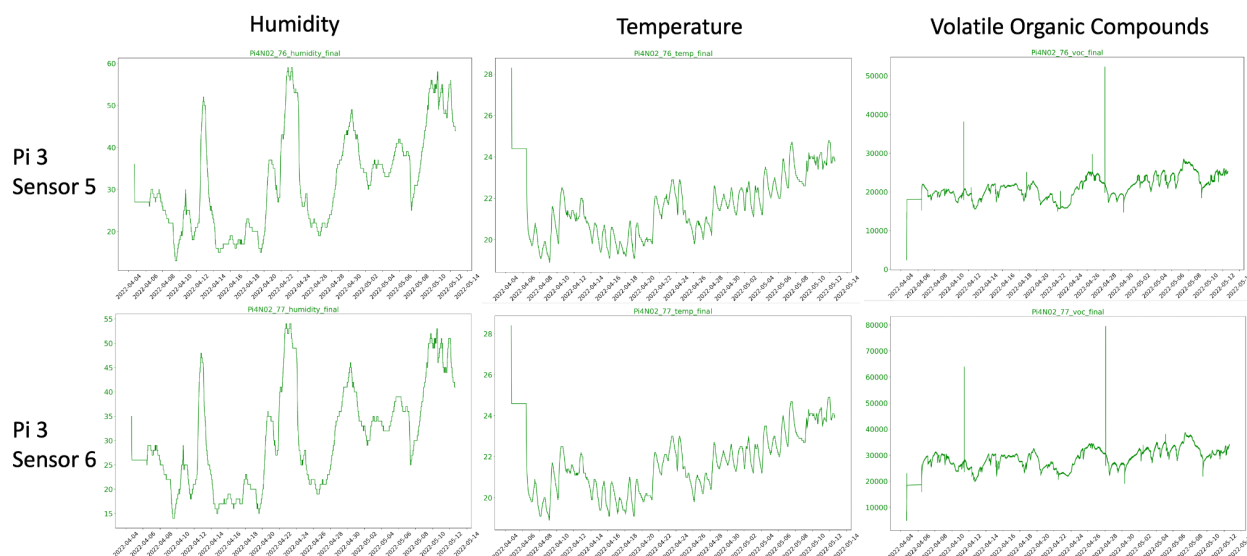


Figure 8: Refrigerated treatment sensor data for two sensors.

The final ambient treatment is included in **Figure 9** and also only includes two sensors for likely the same problem that affected the non-functional PI in the refrigerated case. The temperature and humidity vary more dramatically than the oven or refrigerated cases as expected in an uncontrolled environment and the VOCs in both sensors appear to remain relatively consistent throughout the duration. However, again, the absolute values are not consistent due to the lack of calibration.

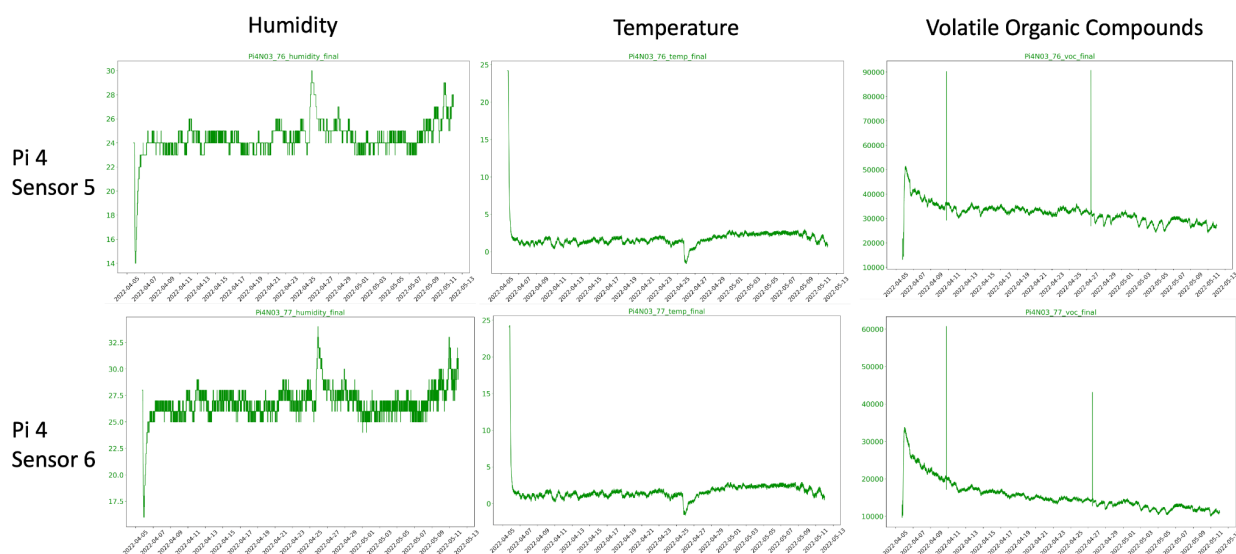


Figure 9: Ambient treatment sensor data for two sensors.

3.4 Flexural strength of specimens

In all eight successfully-read sensors, the values during the 28-day period of humidity and temperatures were averaged for determining the extent of the binder curing which is

hypothesized to be correlated with the final mold strength. **Figure 9** shows the X and Y flexural strengths where X is the direction of inkjetting and Y is the direction of recoating. For both axes, the heated and low humidity case provided improved average strength and the average temperature and humidity over the duration of the experiment had strong correlation but not with statistical significance as the four of the sensors failed to report.. This correlation could be used to provide a threshold to identify the minimum time for curing to provide sufficient strength prior to pouring metal. Future experiments will include measuring conditions for months or years to establish a potential maximum duration for which the molds could be stored prior to use assuming the binder would eventually degrade over time.

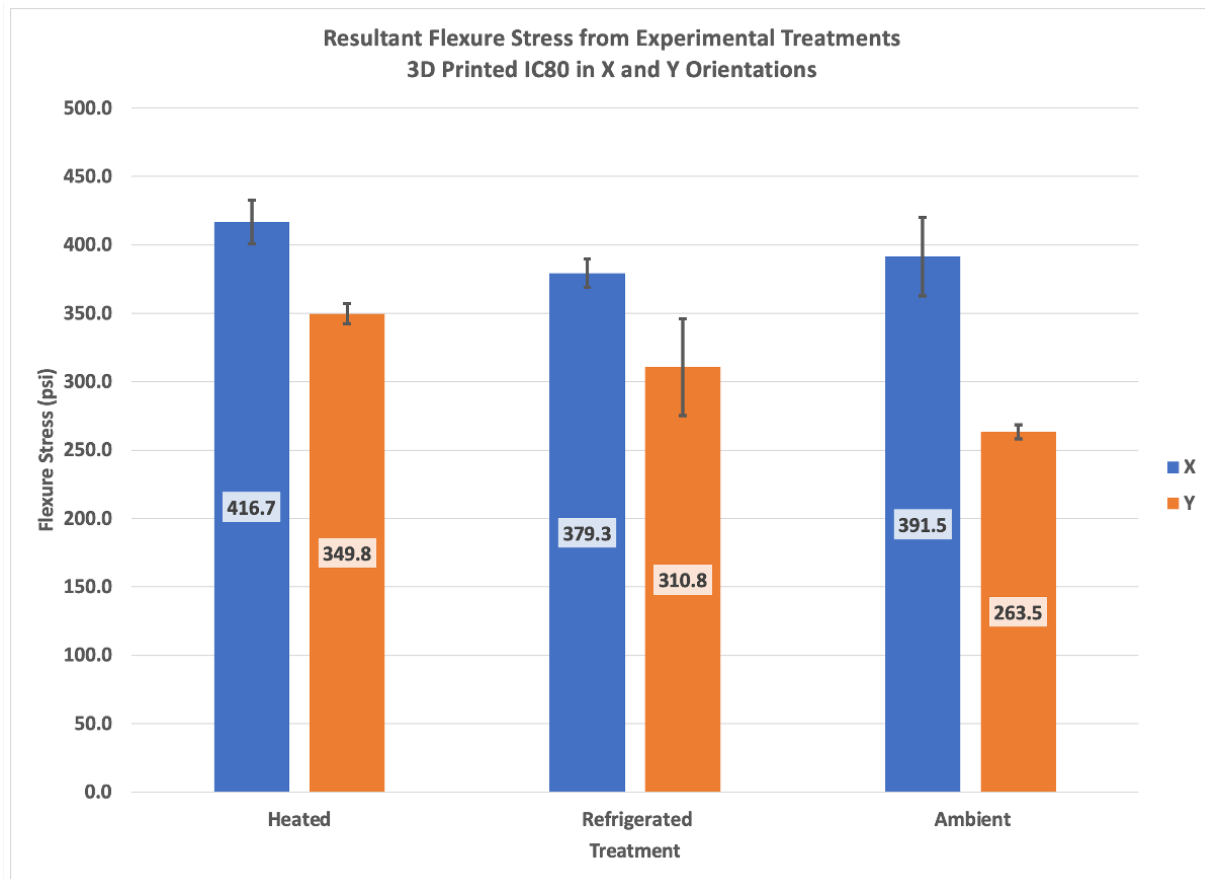


Figure 10: Flexural strength in the X and Y build directions for each of the three treatments: Heated, Refrigerated and Ambient.

4.0 Conclusions

The present experiment has demonstrated the basic utility of monitoring environmental conditions of printed sand molds and cores to ensure that binder was sufficiently cured. This technique will be further explored to establish guidelines for a window in time for which the

molds could be used for casting depending on humidity and temperature. The important conclusion points include:

- Sensors can be embedded successfully within molds during a printer interruption of sand molds to inform the extent of curing,
- For the specific BME680 sensor, the Volatile Organic Compound sensor mode would require calibration to be used in determining if sand binder had sufficiently cured to provide the mold strength required for metal pouring,
- A combined metric of temperature and humidity has been preliminarily shown to provide a higher correlation between the calculated metric and the final mold flexural strength,
- With further experiments, guidelines could be established to allow for the monitoring of temperature and humidity in a mold storage facility to calculate a minimum curing time for any specific conditions, and
- Long-duration experiments will be the focus of future work to understand how long 3D printed sand molds remain sufficiently strong, and if these molds need to have an expiration date with the specific consideration of the environmental conditions that the molds were subjected to in the storage facility over time.

Acknowledgments

We would like to thank the Murchison Endowment at the University of Texas at El Paso and a grant from the American Foundry Society.

References

1. Barnard N. Bronze casting and bronze alloys in ancient China. 1961. Available: <http://www.bcin.ca/Interface/openbcin.cgi?submit=submit&Chinkey=63387>
2. Staff M. Modest Growth in Worldwide Casting Market. Metal Casting Design and Purchasing. 2016.
3. Itc US, Commission USIT, Others. Foundry products: Competitive conditions in the US market. Washington, DC. 2005.
4. Bassoli E, Gatto A, Iuliano L, Violante MG. 3D printing technique applied to rapid casting. Rapid Prototyping Journal. 2007;13: 148–155.
5. Standard A. ISO/ASTM 52900: 2015 Additive manufacturing-General principles-terminology. ASTM F2792-10e1. 2012.
6. Santosh Reddy Sama ,Eric MacDonald, Robert Voigt and Guha Manogharan. Measurement of Metal Velocity in Sand Casting during Mold Filling. Metals . 2019;9. doi:10.3390/met9101079
7. King D, Tansey T. Alternative materials for rapid tooling. J Mater Process Technol. 2002;121: 313–317.
8. Snelling D, Williams C, Druschitz A. A comparison of binder burnout and mechanical characteristics of printed and chemically bonded sand molds. SFF Symposium, Austin, TX. sffsymposium.engr.utexas.edu; 2014. Available: <https://sffsymposium.engr.utexas.edu/sites/default/files/2014-018-Snelling.pdf>
9. Thiel J. Thermal expansion of chemically bonded silica sand. American Foundry society, Schaumburg, IL USA, AFS Proceedings. 2011;1. Available: https://www.sand.org/resource/resmgr/docs/Research/Thiel_Paper.pdf

10. Singh R. Three dimensional printing for casting applications: A state of art review and future perspectives. *Advanced Materials Research. Trans Tech Publ*; 2010. pp. 342–349.
11. Thiel J, Ravi S, Bryant N. Advancements in Materials for Three-Dimensional Printing of Molds and Cores. *Int J Metalcast*. 2017;11: 3–13.
12. Snelling D, Li Q, Meisel N, Williams CB, Batra RC, Druschitz AP. Lightweight Metal Cellular Structures Fabricated via 3D Printing of Sand Cast Molds. *Adv Eng Mater*. 2015;17: 923–932.
13. Snelling D, Blount H, Forman C, Ramsburg K, Wentzel A, Williams C, et al. The effects of 3D printed molds on metal castings. *Proceedings of the Solid Freeform Fabrication Symposium*. 2013. pp. 827–845.
14. Miyanaji H, Zhang S, Yang L. A new physics-based model for equilibrium saturation determination in binder jetting additive manufacturing process. *Int J Mach Tools Manuf*. 2018;124: 1–11.
15. Kang J, Shangguan H, Deng C, Hu Y, Yi J, Wang X, et al. Additive manufacturing-driven mold design for castings. *Additive Manufacturing*. 2018;22: 472–478.
16. Carneiro VH, Rawson SD, Puga H, Meireles J, Withers PJ. Additive manufacturing assisted investment casting: A low-cost method to fabricate periodic metallic cellular lattices. *Additive Manufacturing*. 2020; 101085.
17. Yang L, Harrysson O, Cormier D, West H, Gong H, Stucker B. Additive Manufacturing of Metal Cellular Structures: Design and Fabrication. *JOM*. 2015;67: 608–615.
18. Vuksanovich B, Chavez J, Gygi C, O'Hara R, Cortes P, MacDonald E, et al. Non-Destructive Inspection of Sacrificial 3D Sand-Printed Molds with Geometrically Complex Lattice Cavities. *Int J Metalcast*. 2021. doi:10.1007/s40962-021-00681-w
19. Martof A, Gullapalli R, Kelly J, Rea A, Lamoncha B, Walker JM, et al. Economies of complexity of 3D printed sand molds for casting. 2018 International Solid Freeform Fabrication Symposium. University of Texas at Austin; 2018. Available: <https://repositories.lib.utexas.edu/handle/2152/90082>
20. Walker J, Harris E, Lynagh C, Beck A, Lonardo R. 3D Printed Smart Molds for Sand Casting. *International Journal of*. Available: <https://link.springer.com/article/10.1007/s40962-018-0211-x>
21. Kobliska J, Ostojic P, Cheng X, Zhang X, Choi H, Yang Y, et al. Rapid fabrication of smart tooling with embedded sensors by casting in molds made by three dimensional printing. *Proc SFF Symp*. 2005. pp. 468–475.
22. Walker JM, Prokop A, Lynagh C, Vuksanovich B, Conner B, Rogers K, et al. Real-time process monitoring of core shifts during metal casting with wireless sensing and 3D sand printing. *Additive Manufacturing*. 2019;27: 54–60.
23. Vuksanovich B, Herberger C, Jaric D, Daugherty T, Clancy M, Gaffney S, et al. Wireless Ventilation Measurement in 3D Printed Sand Molds. *Int J Metalcast*. 2021. doi:10.1007/s40962-021-00592-w
24. Parker G, MacDonald E, Zinner T, Yampolskiy M. 3D-Mold'ed In-Security: Mapping Out Security of Indirect Additive Manufacturing. *Proceedings of the 8th ACM on Cyber-Physical System Security Workshop*. New York, NY, USA: Association for Computing Machinery; 2022. pp. 53–61.